The Cryosphere Discuss., 9, 4845–4864, 2015
www.the-cryosphere-discuss.net/9/4845/2015/
doi:10.5194/tcd-9-4845-2015

The Cryosphere Discussions
Open Access

Tomography-based observation of sublimation and snow metamorphism under temperature gradient and advective flow

P. P. Ebner[1,2], **M. Schneebeli**[2], **and A. Steinfeld**[1]

[1]Department of Mechanical and Process Engineering, ETH Zurich, 8092 Zurich, Switzerland
[2]WSL Institute for Snow and Avalanche Research SLF, 7260 Davos-Dorf, Switzerland

Received: 17 August 2015 – Accepted: 21 August 2015 – Published: 11 September 2015

Correspondence to: M. Schneebeli (schneebeli@slf.ch)

Published by Copernicus Publications on behalf of the European Geosciences Union.

Abstract

Snow at or close to the surface commonly undergoes temperature gradient metamorphism under advective flow, which alters its microstructure and physical properties. Time-lapse X-ray micro-tomography is applied to investigate the structural dynamics of temperature gradient snow metamorphism exposed to an advective airflow in controlled laboratory conditions. The sublimation of water vapor for saturated air flowing across the snow sample was experimentally determined via variations of the porous ice structure. The results showed that the exothermic gas-to-solid phase change is favorable vis-a-vis the endothermic solid-to-gas phase change, thus leading to more ice deposition than ice sublimation. Sublimation has a marked effect on the structural change of the ice matrix but diffusion of water vapor in the direction of the temperature gradient counteracted the mass transport of advection. Therefore, the total net ice change was negligible leading to a constant porosity profile. However, the strong reposition process of water molecules on the ice grains is relevant for atmospheric chemistry.

1 Introduction

Snow has a complex porous microstructure and consists of a continuous ice structure made of grains connected by bonds and inter-connecting pores (Löwe et al., 2011). It has a high permeability (Calonne et al., 2012) and under appropriate conditions airflow through the snow structure can occur (Sturm and Johnson, 1991) due to variation of surface pressure (Colbeck, 1989; Albert and Hardy, 1995), simultaneous warming and cooling, and induced temperature gradients (Sturm and Johnson, 1991). Both diffusive and advective airflows affect heat and mass transport in the snowpack and influence chemical concentrations (Gjessing, 1977; Waddington et al., 1996). Various airflow conditions in a snow sample occur, namely: isothermal airflow, temperature gradient along the flow direction, and temperature gradient opposite to the airflow (Fig. 1). Under isothermal condition, the continuous sublimation and deposition of ice due to the

TCD
9, 4845–4864, 2015

Kelvin-effect leads to a saturation of the pore space in the snow (Neumann et al., 2008; Ebner et al., 2014). However, applying a fully isothermal saturated airflow across a snow sample has been shown to have no influence on the coarsening rate that is typical for isothermal snow metamorphism independently of the transport regime in the pores (Ebner et al., 2015a). When applying a temperature gradient, the effect of sublimation and deposition in the snow results from interaction between snow temperature and the local relative humidity in the pores. If vapor is advected from a warmer zone into a colder zone, the air becomes supersaturated, and some water vapor deposits onto the surrounding ice grains. This leads to a change in the microstructure creating whistler-like crystals (Ebner et al., 2015b). The flow rate dependence on the deposition rate of water vapor on the ice matrix was observed, reaching asymptotically a maximum rate of $1.05 \times 10^{-4}\,\mathrm{kg\,m^{-3}\,s^{-1}}$ (Ebner et al., 2015b). Contrarily, if the temperature gradient acts in the opposite direction of the airflow, the airflow through the snow brings cold and relatively dry air into a warmer area, causing that the pore space air becomes undersaturated, and surrounding ice sublimates. Here, we investigate specifically this last effect.

Sublimation of snow is a fundamental process that affects its crystal structure (Sturm and Benson, 1997), and thus is important for ice core interpretation (Stichler et al., 2001), as well as calculation of surface energy balance (Box and Steffen, 2001) and mass balance (Déry and Yau, 2002). Albert (2002) suggest that condensation of water vapor will have a noticeable effect on the microstructure of snow using airflow velocities, vapor transport and sublimation rates calculated using a two-dimensional finite-element model. Neumann et al. (2009) determined that there is no energy barrier to be overcome during sublimation, and suggest that snow sublimation is limited by vapor diffusion into pore space, rather than by sublimation at crystal surface.

In the present work, we studied the surface dynamic of snow metamorphism under an induced temperature gradient and saturated airflow in a controlled laboratory experiments. Sublimation of ice was analyzed by in-situ time-lapse experiments with microcomputer tomography (micro-CT) (Pinzer and Schneebeli, 2009; Chen and Baker,

TCD
9, 4845–4864, 2015

2010; Pinzer et al., 2012; Wang and Baker, 2014; Ebner et al., 2014) to obtain the discrete-scale geometry of snow.

2 Time-lapse tomography experiments

Temperature gradient experiments with fully saturated airflow across snow samples (Ebner et al., 2014) were performed in a cooled micro-CT (Scanco Medical μ-CT80) in a cold laboratory temperature of $T_{\text{lab}} = -15\,^{\circ}\text{C}$. Cold saturated air was blown into the snow samples and warmed up while flowing across the sample. Aluminum foam including a heating wire was used to generate the warm site of the snow, opposite to the entering airflow. We analyzed the following flow rates: a volume flow of 0 (no advection), 0.3, 1.0, and 3.0 $\text{L}\,\text{min}^{-1}$. Higher flow rates were experimentally not possible as shear stresses by airflow destroyed the snow structure (Ebner et al., 2015a). Natural identical snow produced in a cold laboratory (Schleef et al., 2014) was used for the snow sample preparation (water temperature: 30 °C; air temperature: −20 °C). The snow was sieved with a mesh size of 1.4 mm into a box, and was sintered for 27 days at −5 °C to increase the strength and to evaluate the structural change in the earlier stage of metamorphism of new snow. The sample holder (diameter: 53 mm; height: 30 mm) was filled by cutting out a cylinder from the sintered snow and pushing into the sample holder without mechanical disturbance of the core. The snow samples were analyzed over 108 h with time-lapse micro-CT measurements taken every 3 h, producing a sequence of 37 images. The reconstructed micro-CT images were filtered by using a $3 \times 3 \times 3$ median filter followed by a Gaussian filter ($\sigma = 1.4$, support = 3). The Otsu method (Otsu, 1979) was used to automatically perform clustering-based image thresholding to segment the grey-level images into ice and void phase. Morphological properties of the two-phase system were determined based on the exact geometry obtained by the micro-CT. The segmented data were used to calculate a triangulated ice matrix surface and tetrahedrons inscribed into the ice structure. Morphological parameters such as porosity (ε) and specific surface area (SSA) were then calculated.

TCD
9, 4845–4864, 2015

Opening size distribution was applied to extract the mean pore size of each micro-CT scan (d_{mean}) (Haussener et al., 2012). The influence of structural changes on the heat transfer in the snow is analyzed by the effective conductivity k_e (Kaempfer et al., 2005; Petrasch et al., 2008; Calonne et al., 2011). Morphological parameters such as porosity, specific surface area and the initial mean pore size were extracted from the micro-CT pictures to study the ice–air interface dynamic. As additional physical and structural parameter, the thermal conductivity was determined by direct pore-level simulations (DPLS) to determine the influence of changing microstructure (Kaempfer et al., 2005; Petrasch et al., 2008; Calonne et al., 2011; Löwe et al., 2012)

3 Results

Time-lapse tomographic scans were performed with temperature gradients between 43–53 K m^{-1} (Table 1). Small fluctuations of the measured inlet and outlet temperature were due to temperature regulation both inside the cold chamber and inside the micro-CT (Ebner et al., 2014). A shift of $\Delta t < 10$ min between inlet and outlet temperature indicated that a fast equilibrium between the temperature of the snow and the airflow was reached (Albert and Hardy, 1995; Ebner et al., 2015b). The morphological evolution was similar between all four experiments and only a slight rounding and coarsening was visually observed, shown in Fig. 2, indicating that the initial ice grain did not change with time. Only coarsening processes of the ice grain were observed for example, Fig. 3 shows the locations of sublimation and deposition for "ota3" and "ota4". Sublimation of 7.7 and 7.6 % of the ice matrix and deposition of 6.0 and 9.6 % on the ice matrix were observed. The data were extracted by superposition of vertical cross-sections at 0 and 108 h with an uncertainty of 6 %. The mass sublimated preferentially at locations of the ice grain with low radii and was relocated leading to a smoothing of the ice grain and to an increase in the size of pores (Fig. 4a). The pore size increased by 3.4, 3.6, 5.4 and 6.5 % for "ota1", "ota2", "ota3", and "ota4", respectively.

TCD
9, 4845–4864, 2015

Loss of ice of the snow due to sublimation could not be detected by the micro-CT scans and no flow rate dependence was observed during any of the four experiments. The temporal porosity distribution, shown in Fig. 4b, did not change with time and the influence of sublimation of water vapor was not observed. Only "ota2" showed a slight drop in the temporal evolution of the porosity until 18 h into the experiment but kept constant afterwards. This slight drop ($\approx 0.5\,\%$) was probably caused by settling of the snow. A coarsening was observed for each experiment but the influence of changing airflow was not visible, confirmed by the temporal SSA evolution, shown in Fig. 4c.

Although the repositioning of water molecules led to a smoothing of the ice grains, it did not affect the heat transfer in the snow. The thermal conductivity slightly increased after applying airflow to the temperature gradient, shown in Fig. 4d, but no flow rate dependence was observed. Every third scan was used to extract the thermal conductivity and a change of −2.6, 3.6, 2.2, and 2.7 % for "ota1", "ota2", "ota3", and "ota4" was detected.

4 Discussion

The kinetic phase-change from gas to solid is preferable over solid to gas as energy is released rather than consumed leading to more ice deposition rather than ice sublimation. The rate of deposition onto the ice surface depends on the flow rate where warm saturated air cooled down while flowing through the sample, as shown in previous experiments (Ebner et al., 2015b). Its deposition rate asymptotically reached a maximum of $1.05 \times 10^{-4}\,\mathrm{kg\,m^{-3}\,s^{-1}}$. In this study, changing the flow direction lead to a warming up of a cold saturated flow, and resulted in a sublimation rate too small for the analyzed period of the experiment to measure a flow rate dependence by the micro-CT and an influence on the temporal density gradient. A smoothing of ice grains and an increase of the pore space was measured but the airflow velocity did not affect the relocation process of water molecules.

TCD
9, 4845–4864, 2015

A structural change of the ice grains and repositions of water molecules was observed but the total net flux of the snow was not affected. The superposition of vertical cross-section in Fig. 3 shows a big effect on reposition of water molecules on the ice structure. However, the temporal porosity (Fig. 4b) was not affected and the total water vapor net flux was negligible for the analyze volume. Continued sublimation and deposition of water molecules due the Kelvin-effect led to a saturation of the pore space. However, the uptake of water molecules and their transport due to the undersaturated airflow was counteracted by diffusion of water molecules due to the temperature gradient. As thermally induced diffusion was opposite to the airflow gradient, a backflow of water vapor occurred and the two opposite fluxes cancelled each other out. The Peclet numbers, describing the ratio of mass transfer between diffusion and advection, measured during each experiment, showed that diffusion was still dominant (Table 1), thus indicating that water molecules were transported back and forth due to diffusive and advective transport.

As a Peclet higher than 1 is not possible in nature (Ebner et al., 2015a), sublimation inside a snowpack has a significant influence not on the total net mass change but on the structural orientation of the ice grains due to redistribution of water vapor on the ice matrix. Also the increasing pore size has an influence on the flow field leading to a deceleration of the flow and therefore the interaction of an air-parcel with the ice matrix in the pores increases. In addition, the diffusive transport rises whereas the advective transport decreases changing the mass transport in the pores. Our results support the hypothesis of Neumann et al. (2009) that sublimation is limited by vapor diffusion into the pore space rather than sublimation at crystals faces. This is also supported by the temporal evolution of the porosity (Fig. 4b) and the SSA (Fig. 4c), as no velocity dependence was observed and the structural changes were too small to be detected by the micro-CT.

The influence of diffusion of water vapor in the direction of the temperature gradient and the influence of the residence time of an air-parcel in the pores were also confirmed by a low mass change at the ice–air interface. Overlapping two consecutive 3-D

TCD
9, 4845–4864, 2015

images, the order of magnitude of freshly sublimated ice was detected. The absolute mass change at the ice–air interface ($kg\,m^{-3}\,s^{-1}$) estimated by the experimental results is defined as

$$S_{m,\,exp} = \left| \rho_i \frac{\Delta(1-\varepsilon)}{\Delta t} \right| \quad (1)$$

where $\Delta(1-\varepsilon)$ is the change in the porosity between two images separated by the time step Δt, and ρ_i is the density of ice. Albert and McGilvary (1992) and Neumann et al. (2009) presented a model to calculate sublimation rates directly in an aggregate snow sample

$$S_m = |h_m SA_V(\rho_{sat} - \rho_v)| \quad (2)$$

where SA_V is the specific surface area per volume of snow, and h_m is the mass-transfer coefficient ($m\,s^{-1}$) given by (Neumann et al., 2009)

$$h_m = (0.566 \times Re + 0.075) \times 10^{-3} \quad (3)$$

assuming that the sublimation occurs within the first few mm of the sample. Re is the corresponding Reynolds-number of the flow. The absolute sublimation rate is driven by the difference between the local vapor density (ρ_v) and the saturation vapor density (ρ_{sat}) (Neumann et al., 2009; Thorpe and Mason, 1966). Table 2 shows the estimated absolute sublimation rate by the experiment (Eq. 1) and the model (Eq. 2). The very small change in porosity due to densification during the first 18 h for "ota2" was not taken into account. The estimated sublimation rates by the experiment were two orders of magnitude lower than the modelled values and also two orders of magnitude lower than for the temperature gradient along an airflow experiment (Ebner et al., 2015b). As the air in the pore spaces are always saturated (Neumann et al., 2009), the back diffusion of water vapor in the direction of the temperature gradient led to a lower mass transfer rate of sublimation. The flow rate dependence for the model described

TCD
9, 4845–4864, 2015

is shown by the mass-transfer coefficient (Eq. 3), increasing with higher airflow. However, the values calculated from the experiment showed a different trend. Increasing the flow rate led to a lower mass transfer rate due to a lower residence time of the air in the pores. Transfer of heat toward and water vapor away from the sublimating interface may also limit the sublimation rate. In general, the results of the model by Neumann et al. (2009) have to be interpreted with care, as the model was set up to saturate dry air under isothermal conditions. Ice crystals sublimated as dry air enters the snow sample; water vapor was advected throughout the pore space by airflow until saturation vapor pressure was reached, preventing further sublimation. The model by Neumann et al. (2009) does not consider the influence of a temperature gradient and the additional vapor pressure gradient was not analyzed.

In the experiments by Neumann et al. (2009), sublimation of snow using dry air under isothermal condition showed a temperature drop for approximately the first 15 min after sublimation began and stayed constant because the latent heat absorption of sublimation for a given flow rate and heat exchange with the sample chamber equalized each other. Such a temperature drop was not observed in our experiments. In the experiments by Neumann et al. (2009) the amount of energy used for sublimation was between -10 and $-40\,\mathrm{J\,min^{-1}}$ for saturation of dry air. Using the expected mass change at the ice–air interface $S_{\mathrm{m,\,exp}}$ (Eq. 1) and the latent heat of sublimation ($L_{\mathrm{sub}} \approx 2834.1 \times 10^3\,\mathrm{J\,kg^{-1}}$) the energy needed for sublimation ranged between -2 and $-12\,\mathrm{J\,min^{-1}}$ for our experiments. Our estimated values are a factor up to five lower than the estimated numbers of Neumann et al. (2009), because the entering air was already saturated (with reference to the cold temperature) at the inlet. The needed energy for sublimation could be balanced between the sensible heat carried into and out of the sample, and the exchange of the snow sample with the air stream and the surrounding prevented a temperature drop.

Thermal conductivity changed insignificantly in these experiments. This indicates that advective cold airflow opposite to a temperature gradient reduces or suppresses

TCD
9, 4845–4864, 2015

the increase in thermal conductivity usually observed by temperature gradient metamorphism (Riche and Schneebeli, 2013).

5 Summary and conclusion

We performed four experiments of temperature-gradient metamorphism of snow under saturated advective airflow during 108 h. Cold saturated air was blown into the snow samples and warmed up while flowing across the sample. The temperature gradient varied between 43 and 53 $K m^{-1}$ and the snow microstructure was observed by X-ray micro-tomography every 3 h. The micro-CT scans were segmented, and porosity, specific surface area, and the mean pore-size were calculated. Effective thermal conductivity was calculated in direct pore-level simulations (DPLS).

Compared to deposition (shown in Ebner et al., 2015b), sublimation showed a small effect on the structural change of the ice matrix. A change in the pore size was most likely due to sublimation of ice crystal with low radii but a significant loss of water molecules of the snow sample and mass transfer away from the ice interface due to sublimation and advective transport could not be detected by the micro-CT scans and no flow rate dependence was observed. The interaction of mass transport of advection and diffusion of water vapor in the direction of the temperature gradient and the influence of the residence time of an air-parcel in the pores led to a negligible total mass change of the ice. However, a strong reposition of water molecules on the ice grains was observed.

The kinetic phase-change from gas to solid is preferable as energy is released compared to solid to gas where energy is required, thus leading to more water molecule deposition than water molecule sublimation. The energy needed for sublimation was too low to see a significant temperature drop because the needed energy was balanced between the sensible heat carried into and out of the sample, and the exchange of the snow sample with the air stream and the surrounding.

TCD
9, 4845–4864, 2015

This is the third paper of a series analyzing an advective airflow in a snowpack. Previous work showed that: (1) under isothermal conditions Kelvin-effect leads to a saturation of the pore space in the snow but did not affect the structural change (Ebner et al., 2015a), (2) applying a temperature gradient along the flow direction leads to a change in the microstructure and creation of whistler-like structures due to deposition of water molecules on the ice matrix (Ebner et al., 2015b), and (3) a temperature gradient opposed to the flow had a negligible total mass change of the ice but a strong reposition effect of water molecules on the ice grains, shown in this paper. Conditions (1) and (3) showed that they have a negligible effect on the structural changes of the ice matrix and can be neglected to improve models for firn compaction and evolution. In contrast, conditions (2) showed a significant impact on the structural evolution and seem to be essential for such snowpack models and other numerical simulations. Nevertheless, the strong reposition of water molecules on the ice grains observed for all conditions (1)–(3) can have a significant impact on atmospheric chemistry.

The Supplement related to this article is available online at doi:10.5194/tcd-9-4845-2015-supplement.

Acknowledgements. The Swiss National Science Foundation granted financial support under project Nr. 200 020–146 540. The authors thank M. Jaggi, S. Grimm, H. Löwe for technical and modelling support.

References

Albert, M. R.: Effects of snow and firn ventilation on sublimation rates, Ann. Glaciol., 35, 52–56, 2002.

Albert, M. R. and Hardy, J. P.: Ventilation experiments in a seasonal snow cover, in: Biogeochemistry of Seasonally Snow-Covered Catchments, IAHS Publ. 228, edited by: Tonnessen, K. A., Williams, M. W., and Tranter, M., IAHS Press, Wallingford, UK, 41–49, 1995.

TCD
9, 4845–4864, 2015

Albert, M. R. and McGilvary, W. R.: Thermal effects due to air flow and vapor transport in dry snow, J. Glaciol., 38, 273–281, 1992.
Box, J. E. and Steffen, K.: Sublimation on the Greenland ice sheet from automated weather station observations, J. Geophys. Res., 107, 33965–33981, 2001.
Calonne, N., Flin, F., Morin, S., Lesaffre, B., and Rolland du Roscoat, S.: Numerical and experimental investigations of the effective thermal conductivity of snow, Geophys. Res. Lett., 38, 1–6, 2011.
Calonne, N., Geindreau, C., Flin, F., Morin, S., Lesaffre, B., Rolland du Roscoat, S., and Charrier, P.: 3-D image-based numerical computations of snow permeability: links to specific surface area, density, and microstructural anisotropy, The Cryosphere, 6, 939–951, doi:10.5194/tc-6-939-2012, 2012.
Chen, S. and Baker, I.: Evolution of individual snowflakes during metamorphism, J. Geophys. Res., 115, 1–9, 2010.
Colbeck, S. C.: Air movement in snow due to windpumping, J. Glaciol., 35, 209–213, 1989.
Déry, S. J. and Yau, M. K.: Large-scale mass balance effects of blowing snow and surface sublimation, J. Geophys. Res., 107, 4679, doi:10.1029/2001JD001251, 2002.
Ebner, P. P., Grimm, S. A., Schneebeli, M., and Steinfeld, A.: An instrumented sample holder for time-lapse microtomography measurements of snow under advective airflow, Geosci. Instrum. Method. Data Syst., 3, 179–185, doi:10.5194/gi-3-179-2014, 2014.
Ebner, P. P., Schneebeli, M., and Steinfeld, A.: Tomography-based monitoring of isothermal snow metamorphism under advective conditions, The Cryosphere, 9, 1363–1371, doi:10.5194/tc-9-1363-2015, 2015a.
Ebner, P. P., Andreoli, C., Schneebeli, M., and Steinfeld, A.: Tomography-based observation of ice–air interface dynamics of temperature gradient snow metamorphism under advective conditions, J. Geophys. Res., submitted, 2015b.
Gjessing, Y. T.: The filtering effect of snow, in: Isotopes and Impurities in Snow and Ice Symposium, edited by: Oeschger, H., Ambach, W., Junge, C. E., Lorius, C., and Serebryanny, L., 118, IASH-AISH Publication, Dorking, 199–203, 1977.
Haussener, S., Gergely, M., Schneebeli, M., and Steinfeld, A.: Determination of the macroscopic optical properties of snow based on exact morphology and direct pore-level heat transfer modeling, J. Geophys. Res., 117, 1–20, 2012.
Kaempfer, T. U., Schneebeli, M., and Sokratov, S. A.: A microstructural approach to model heat transfer in snow, Geophys. Res. Lett., 32, 1–5, 2005.

TCD
9, 4845–4864, 2015

Löwe, H., Spiegel, J. K., and Schneebeli, M.: Interfacial and structural relaxations of snow under isothermal conditions, J. Glaciol., 57, 499–510, 2011.
Löwe, H., Riche, F., and Schneebeli, M.: A general treatment of snow microstructure exemplified by an improved relation for thermal conductivity, The Cryosphere, 7, 1473–1480, doi:10.5194/tc-7-1473-2013, 2013.
Neumann, T. A., Albert, M. R., Lomonaco, R., Engel, C., Courville, Z., and Perron, F.: Experimental determination of snow sublimation rate and stable-isotopic exchange, Ann. Glaciol., 49, 1–6, 2008.
Neumann, T. A., Albert, M. R., Engel, C., Courville, Z., and Perron, F.: Sublimation rate and the mass-transfer coefficient for snow sublimation, Int. J. Heat Mass Trans., 52, 309–315, 2009.
Otsu, N.: A threshold selection method from gray-level histograms, IEEE T. Syst. Man Cyb., 9, 62–66, 1979.
Petrasch, J., Schrader, B., Wyss, P., and Steinfeld, A.: Tomography-based determination of effective thermal conductivity of fluid-saturated reticulate porous ceramics, J. Heat Transf., 130, 1–10, 2008.
Pinzer, B. R. and Schneebeli, M.: Snow metamorphism under alternating temperature gradients: morphology and recrystallization in surface snow, Geophys. Res. Lett., 36, 1–4, 2009.
Pinzer, B. R., Schneebeli, M., and Kaempfer, T. U.: Vapor flux and recrystallization during dry snow metamorphism under a steady temperature gradient as observed by time-lapse microtomography, The Cryosphere, 6, 1141–1155, doi:10.5194/tc-6-1141-2012, 2012.
Riche, F. and Schneebeli, M.: Thermal conductivity of snow measured by three independent methods and anisotropy considerations, The Cryosphere, 7, 217–227, doi:10.5194/tc-7-217-2013, 2013.
Schleef, S., Jaggi, M., Löwe, H., and Schneebeli, M.: Instruments and Methods: an improved machine to produce nature-identical snow in the laboratory, J. Glaciol., 60, 94–102, 2014.
Stichler, W., Schotterer, U., Frohlich, K., Ginot, P., Kull, C., Gäggeler, H., and Pouyaud, P.: Influence of sublimation on stable isotope records recovered from high-altitude glaciers in the tropical Andes, J. Geophys. Res., 106, 22613–22630, 2001.
Sturm, M. and Benson, C.: Vapor transport grain and depth-hoar development in the subarctic snow, J. Glaciol., 43, 42–59, 1997.
Sturm, M. and Johnson, J. B.: Natural convection in the subarctic snow cover, J. Geophys. Res., 96, 11657–11671, 1991.

TCD
9, 4845–4864, 2015

Thorpe, A. D. and Mason, B. J.: The evaporation of ice spheres and ice crystals, Brit. J. Appl. Phys., 17, 541–548, 1966.
Waddington, E. D., Cunningham, J., and Harder, S. L.: The effects of snow ventilation on chemical concentrations, in: Chemical Exchange Between the Atmosphere and Polar Snow, NATO ASI Series 43, edited by: Wolff, E. W. and Bales, R. C., Springer, Berlin, 403–452, 1996.
Wang, X. and Baker, I.: Evolution of the specific surface area of snow during high-temperature gradient metamorphism, J. Geophys. Res.-Atmos., 119, 13690–13703, 2014.

TCD
9, 4845–4864, 2015

Table 1. Morphological and flow characteristics of the experiments: volume flow ($\dot{V}$), initial superficial velocity in snow ($u_{D,0}$), initial snow density (ρ_0), initial porosity (ε_0), specific surface area (SSA_0), initial mean pore size (d_{mean}), average inlet ($T_{in,\,ave}$) and outlet temperature ($T_{out,\,ave}$), and the average temperature gradient (∇T_{ave}), corresponding Reynolds number (Re) and Peclet number (Pe).

Name	$\dot{V}$ $L\,min^{-1}$	$u_{D,0}$ $m\,s^{-1}$	ρ_0 $kg\,m^{-3}$	ε_0 –	SSA_0 $m^2\,kg^{-1}$	d_{mean} mm	$T_{in,\,ave}$ °C	$T_{out,\,ave}$ °C	∇T_{ave} $K\,m^{-1}$	Re –	Pe –
ta1	–	–	284.3	0.69	25.0	0.30	−13.8	−12.5	43.3	–	–
ta2	0.3	0.004	256.8	0.72	26.3	0.33	−14.0	−12.5	50.0	0.07	0.05
ta3	1.0	0.012	256.8	0.72	24.3	0.34	−13.8	−12.3	43.3	0.25	0.19
ta4	3.0	0.036	265.9	0.71	21.7	0.36	−14.6	−13.0	53.3	0.78	0.61

TCD
9, 4845–4864, 2015

Table 2. Estimated sublimation rate S_m using the mass transfer coefficient h_m determined by Neumann et al. (2009) and the corresponding average surface area per volume $SA_{V,ave}$. S_m can be compared with the measured sublimation rate of the experiment $S_{m,\,exp}$ (Eq. 1).

Name	$SA_{V,ave}$ mm^{-1}	h_m $m\,s^{-1}$	S_m $kg\,m^{-3}\,s^{-1}$	$S_{m,\,exp}$ $kg\,m^{-3}\,s^{-1}$
ta1	22.44	0.75×10^{-4}	4.83×10^{-4}	0.68×10^{-6}
ta2	23.98	1.15×10^{-4}	2.99×10^{-4}	4.48×10^{-6}
ta3	21.88	2.17×10^{-4}	5.15×10^{-4}	0.76×10^{-6}
ta4	19.61	5.16×10^{-4}	10.9×10^{-4}	0.08×10^{-6}

TCD
9, 4845–4864, 2015

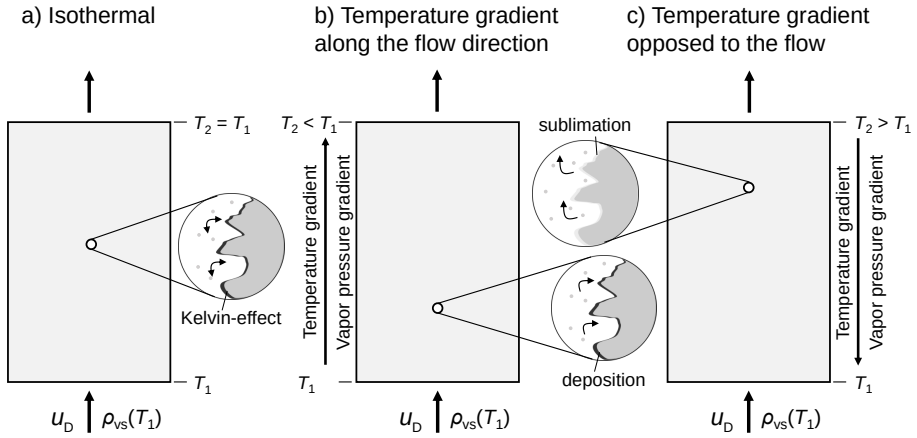

Figure 1. Schematic of the ice–air interface transport processes: **(a)** under isothermal conditions Kelvin-effect leads to a saturation of the pore space in the snow but did not affect the structural change (Ebner et al., 2015a); **(b)** temperature gradient along the flow direction leads to a change in the microstructure due to deposition (Ebner et al., 2015b); **(c)** temperature gradient opposite to the flow has a negligible total mass change of the ice but a strong reposition effect of water molecules on the ice grains, shown in this paper.

TCD
9, 4845–4864, 2015

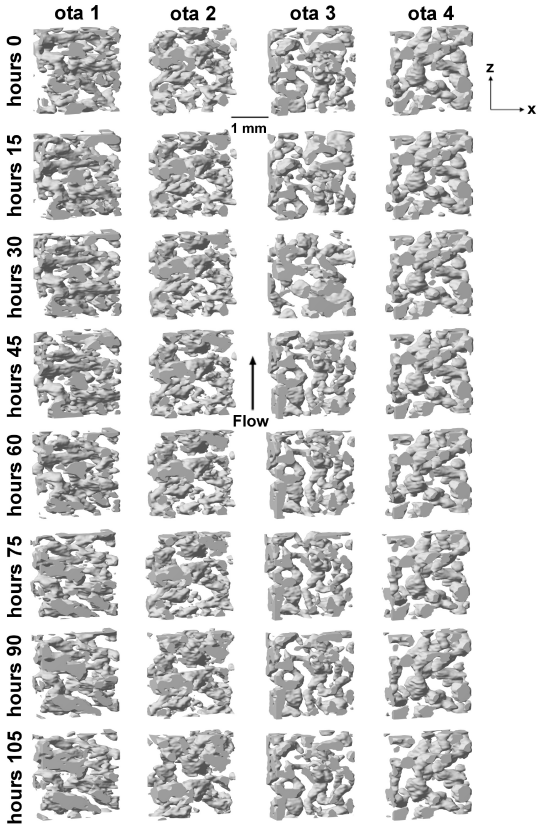

Figure 2. Evolution of the 3-D structure of the ice matrix with applied temperature gradient and advective conditions. Experimental conditions (from left to right) at different measurement times from beginning to the end (top to bottom) of the experiment. The shown cubes are 110×40×110 voxels (2 mm × 0.7 mm × 2 mm) large (a high resolution figure can be found in Supplement).

TCD
9, 4845–4864, 2015

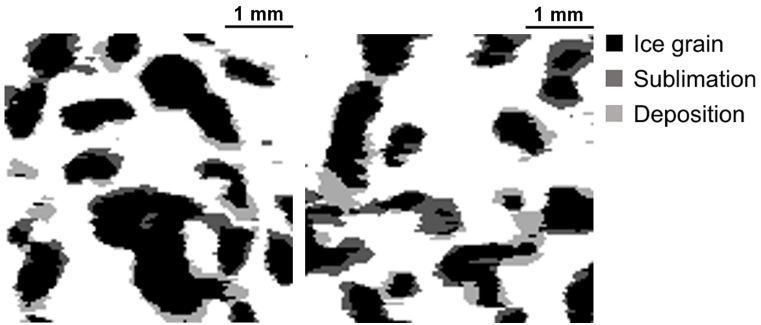

Figure 3. Superposition of vertical cross-section parallel to the flow direction at time 0 and 108 h for (left panel) “ota3” and (right panel) “ota4”. Sublimation and deposition of water vapor on the ice grain were visible with an uncertainty of 6 % (a high resolution figure can be found in Supplement).

TCD
9, 4845–4864, 2015

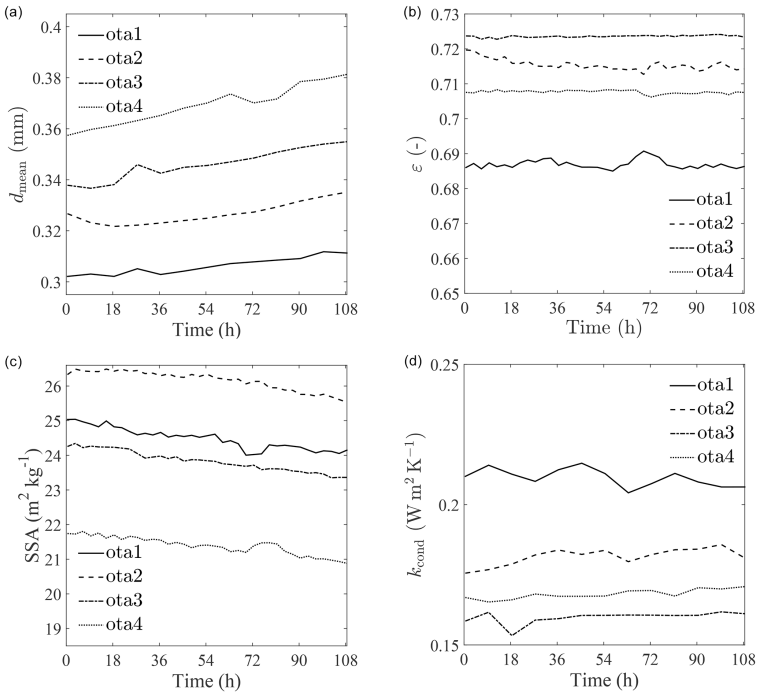

Figure 4. Temporal evolution of **(a)** the mean pore size, d_{mean}, of the snow samples obtained by opening-size distribution the porosity obtained by triangulated structure surface method, **(c)** the specific surface area, SSA, of the ice matrix obtained by triangulated structure surface method, and **(d)** the effective conductivity of the snow sample estimated by DPLS simulations.

TCD
9, 4845–4864, 2015